Distribution of suspended particulate matter at the equatorial transect in the Atlantic Ocean

Vadim Sivkov[1, 2] and Ekaterina Bubnova[1, 2]

[1]Shirshov Institute of Oceanology, Russian Academy of Sciences, 36, Nahimovskiy prospekt, Moscow, Russia, 117997
[2]Immanuel Kant Baltic Federal University, Kaliningrad, 14, A. Nevskogo str., Kaliningrad, Russia, 236016

Correspondence: Ekaterina Bubnova (bubnova.kat@gmail.com)

Abstract. ~~Studied~~ A studied oceanographic transect across the Equatorial Atlantic is considered as "screenshot~~"~~" of suspended particulate matter distribution against a hydrographical background. ~~The~~ An area of abnormal high suspended matter volume concentrations was found above the Sierra Leone Rise from top to bottom (eastern part of the transect). The suggested explanation for the anomaly is based on the ballast hypothesis whereby solid particles are incorporated as ballast into suspended biogenic aggregates, leading to increased velocities of sinking. This process is located within the Northwest African upwelling area, since the plankton exposed to the Saharan dust abundance form a significant number of aggregates ~~lately~~ recently transported equatorward via Canary Current. ~~The~~ An intermediate nepheloid layer associated with the Deep Western Boundary Current was recorded from the South American Slope at ~~the~~ depths of 3200–3700 m to ~~the depth of~~ 4300 m above the Para Abyssal Plain. Antarctic Bottom Water enriched in suspended matter was found mostly in the troughs at 40–41° W. It was detached from the bottom, coinciding with the core of the flow due to the bottom rise ~~("dam"~~"dam") located up-stream. The grain size of particles ~~was in accordance with polymodal distribution — the~~ has a polymodal distribution with 2–4 μm and ~~the~~ 8–13 μm modes. The registered rise in percentage of the 7–21 μm-sized particles suggests the presence of the well-known coarse mode (20–60 μm) formed by aggregation of transparent exopolymer particles (mucus).

1 Introduction

Numerous studies have focused on characterizing the suspended particulate matter (SPM) during the past half a century due to the fact of its importance. Modern understanding of the basic patterns of the SPM distribution in the ocean had emerged by the end of the 1980s (Chester, 1990). Therefore, the oceanic SPM spread may be depicted as a three-layer structure with following layers (a) a surface water, (b) a clear water minimum, and (c) a deep-water ~~(Biscaye and Eittreim, 1977; Chester, 1990)~~(Biscaye and Eittrein
It was also indicated that the distribution of the SPM in oceans shows basically the interaction between the bottom sediments and abyssal waters movement, so SPM-rich benthic nepheloid layers (BNLs) coincide with pathways of the western boundary currents (Biscaye and Eittreim, 1977). The works of Armi (1978) and McCave (1983) pointed out the lateral advection of SPM, that occurs due to detaching of bottom mixed layers from the slope and leads to thickening and layering of BNLs. There are also strong intermediate nepheloid layers (INLs) in the clear water minimum layer in some regions (Thorpe and White, 1988).

The Geochemical Ocean Transects study (GEOSECS) ~~has introduced a first description of the suspended particles~~ introduced an early description of suspended particle distribution in the ocean, ~~taking into account mostly~~ using mostly data on SPM collected via filtration (Craig and Turekian, 1976). The three-layer model of the SMP concentration distribution was also successively described in (Brewer et al., 1976) at a transect through the western Atlantic Ocean: high concentrations were found in surface and in rapidly moving bottom waters, while low concentrations were observed in the mid-water regions of the sub-tropical gyres.

The SPM plays a crucial role in both regulation ~~the~~ of sea water composition and material transport throughout the entire water column, experiencing various processes (e.g. dissolution, decomposition, disaggregation, aggregation, etc.) (Gardner et al., 1985a). It was shown ~~(McCave, 1975)~~ by McCave (1975) that the SPM sizes follow a hyperbolic distribution with increase of ~~the fine particles abundance, whereby~~ fine particle abundance, whereas most of the particle flux to the bottom lies in the coarser size classes.

Sinking particles may remove the dissolved trace elements from solution (Lal, 1977) and transport them to bottom sediments. The extent to which the behavior of dissolved trace elements is dominated by suspended solids was referred as the great particle conspiracy (Turekian, 1977).

The summary in (Jeandel et al., 2015) shows that fine particles (<53 μm) represent the vast majority of particles in the ocean. According to (Sheldon et al., 1972) the size spectrum of small particles varies predictably both geographically and with depth. A linkage of strong BNLs and bentic storms with upper ocean dynamic was described in (Gardner et al., 2018). Yet the full characterization of fine SPM distribution and composition in the ocean remains studied insufficiently due to the high research costs. Thus, ~~the transect research of the~~ research on transects of fine SPM distribution are still ~~demanded~~required.

The Equatorial Atlantic is ~~the~~ an area of increased oceanographic interest owing to the central position on the global circulation map. The aim of this study was to explain the distribution of fine SPM concentration and size spectra ~~at the~~ on a transatlantic oceanographic transect in the equatorial zone of the Atlantic Ocean (Ioffe-2000 transect). The hydrophysical and hydrochemical data (background for the SPM distribution) have been published in sufficient detail (Sokov et al., 2002; Sarafanov et al., 2007). The SPM data, on the contrary, have been published only briefly (Sivkov et al., 2001) due to the ~~significant differences between the obtained data and the currently accepted conception on this matter~~ fact that not all the peculiarities were in accordance with general knowledge (Biscaye and Eittreim, 1977). So far, the ideas have been formed to explain the features of the SPM distribution obtained on the transect.

2 Materials and Methods

A sublatitudinal transect (13–28 July 2000) between the continental slopes of Guinea and Brazil with ~~closely spaced 61~~ 61 closely spaced stations was performed during the 8th cruise of the R/V ~~*Akademik Ioffe*~~ Akademik Ioffe (Fig. 1). Additional surface samples of SPM were taken in the Northwest African upwelling zone (Cap Blanc area) just before the transect conduction (10–11 July 2000). Sampling at the Ioffe-2000 transect was carried out using the hydrological complex, ~~equiped~~ equipped with 5 L Niskin bottles, while the additional surface sampling was carried out with a use of plastic bucket.

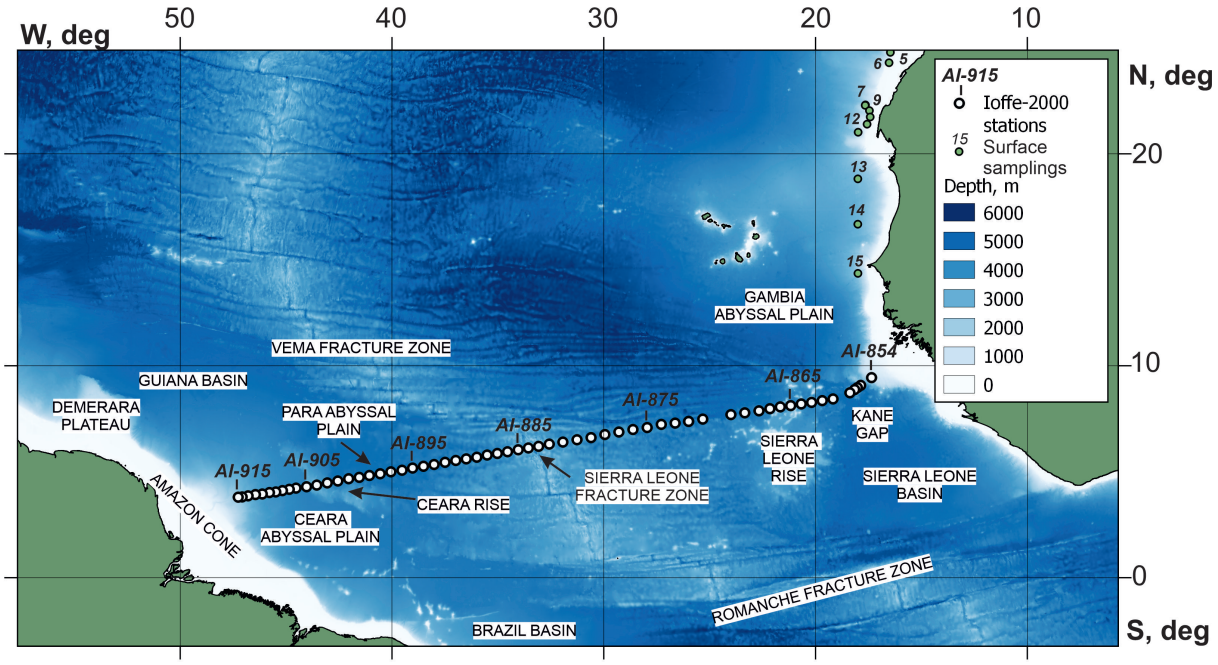

Figure 1. The Ioffe-2000 transect position in the study area (station numbers, every 10 stations). Bottom topography taken according to ~~(GEBCO Bathymetric Compilation Group, 2020)~~GEBCO Bathymetric Compilation Group (2020).

The SPM volume concentration and particle size distribution were determined by the conductometric method via the Coulter counter (~~Z_{bi}~~ Zbi model) for 407 samples from the Ioffe-2000 transect and 13 samples from the Cap Blanc area (Supplement 1). The Coulter counter calibration was carried out using Coulter Electronics standard methodology using 5.96 μm diameter latex particles. The 70 μm aperture was used, which ensured counting of particles in the size range of 1.8–20.7 μm. Volume suspended solids concentration and size distribution were calculated based on the assumption of particle sphericity. The distributions of temperature, salinity, dissolved oxygen and silicates on the transect (Sokov et al., 2002; Sarafanov et al., 2007) were used in relation to the SPM data. The temperature and salinity data were recorded via an Neil Brown Mark-III CTD profile (accuracy of measurements was 0.002°C for temperature, 0.002 psu for salinity). The temperature accuracy was determined via precruise and postcruise laboratory calibrations, and the salinity accuracy was calculated by comparison with the bottle data. Water samples for additional salinity measurement and silicate concentrations were obtained using the hydrological complex mentioned above at every station. The silicate concentrations were determined according to the standard method (Mullin and Riley, 1955) (with the accuracy better than 0.2 μmol kg^{-1}) (Sokov et al., 2002; Sarafanov et al., 2007).

3 Hydrographical settings

3.1 Upper ocean

The upper levels of the Equatorial Atlantic water structure are dominated by the presence of large-scale westward currents and eastward countercurrents (Fig. 2A). The northern part of the studied region includes an eastward flowing North Equatorial Countercurrent (NECC) at depths 0–100 m and the North Equatorial Undercurrent (NEUC) at depths between 100 m and 300 m (Wilson et al., 1994; Bischof et al., 2003), a westward flowing North Equatorial Current (NEC) and South Equatorial Current (SEC) (Bourlès et al., 1999).

The North Brazil Current (NBC) is a major western boundary current in the Atlantic Ocean, that transports water to the north across the equator within the upper 300 m ~~(Johns et al., 1998; Bischof et al., 2003)~~(Johns et al., 1998; Bischof et al., 2003). The NBC starts as a northern branch of water originating from the SEC as it bifurcates nearby the Brazilian continental shelf at about 10° S, which turns the SEC to the north, and then it merges with the North Brazil Undercurrent (NBUC). The NBC passes the equator, ~~caring~~ carrying Tropical Surface Water (TSW, ~~mixed surface~~ surface mixed layer) at ~~the~~ depths of 0–100 m ~~depth~~ and the upper part of South Atlantic Central Water (SACW) (100–500 m). There is also ~~the~~ Salinity Maximum Water on the boundary of these two water masses, that was formed in the central subtropical gyre (Stramma et al., 2005). General patterns of the western north equatorial circulation, according to ~~(Bruce et al., 1985)~~Bruce et al. (1985), include a large anticyclonic eddy (diameter approximately 300–400 km) ~~to the 7–10~~at 7–10° N and a southern eddy-like feature (3–6° N). Anticyclonic eddy features exist in the NBC upstream from the retroflection (Johns et al., 1998) and they may propagate downstream within the NBC and serve as a catalyst for NBC ring shedding.

The NBC divides into both surface and subsurface layers of the NECC/NEUC system (Wilson et al., 1994). There are three possible pathways for continuation of the NBC upper part (0–100 m) to the north: the coastal boundary current (Csanady, 1985; Candela et al., 1992), rings from the NBC retroflection (Didden and Schott, 1993; Richardson et al., 1994; Fratantoni et al., 1995; Johns et al., 1998), and offshore retroflection of the current into the NECC (Mayer and Weisberg, 1993). The NECC lies between 3° N and 10° N, roughly considered to be the northern boundary for the SEC (Peterson and Stramma, 1991; Bourlès et al., 1999). Both the NECC and the SEC are the strongest from July to September and are also at their northernmost positions during this time (Peterson and Stramma, 1991). The retroflection of the NBC is considered to be the main source of the NECC (Wilson et al., 1994; Bourlès et al., 1999; Schott et al., 2002), while additional sources for the latter are both the retroflected NEC transport and the northern branch of the SEC (Wilson et al., 1994). The thermocline NBC flow (in the 100–300-m layer) could also feed the NEUC between 2° N and 5° N (Johns et al., 1998). Some of thermocline flow of the NEUC may also recirculate back into the NBC by means of the semipermanent anticyclonic "Amazon~~" eddy centered~~ " eddy centred near 2° N (Bruce et al., 1985).

Caused by the Atlantic trade wind belt, the NEC is found in the North Atlantic from about 7° N to about 20° N (Schott et al., 2002) and is a broad westward flowing current that forms the southern limb of the North Atlantic subtropical gyre (Bourlès et al., 1999). The Guinea Dome (GD) is a permanent thermal upwelling dome (Rossignol and Meyrueis, 1964) centered at 9° N, 25° ~~W and~~ Wand at 10.5° N, 22° W in boreal summer and winter ~~accordingly~~ respectively (Siedler et al., 1992). The main

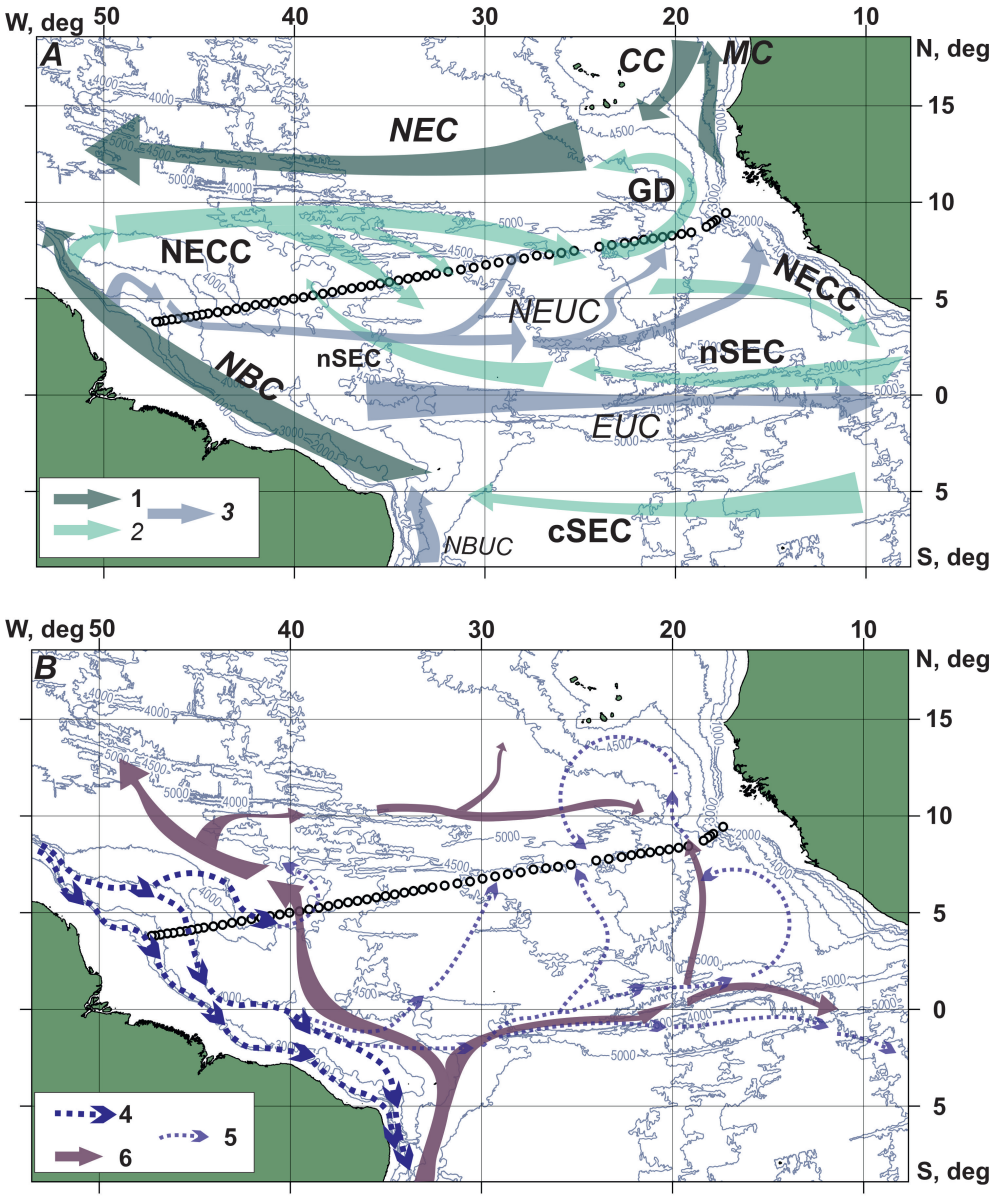

Figure 2. Generalized circulation schematics within the study area: surface and subsurface layers (A) and ~~intermediate,~~ deep ~~,~~and bottom layers (B), where 1 — surface currents (from 0 up to 100 m), 2 — subsurface currents (from 100 up to 500 m), 3 — ~~deep~~ joint surface and subsurface currents (from 0 up to 500 m), 4 — the Deep Western Boundary Current (DWBC) cores, 5 — schematic DWBC recirculation, ~~6~~ —6— AABW. The references and current abbreviations are explained in the text. ~~Isobaths every 500 m~~White circles — Ioffe-2000 transect stations.

existence conditions for GD ~~existence is~~ are a cyclonic circulation composed of the eastward NECC and NEUC along with the westward NEC (Stramma and Schott, 1999).

According to Mittelstaedt (1991), reaching the African coast, the NECC bifurcates and a part of its flow goes northwards, forming the Mauritania Current (MC). The summer — early autumn relaxation of the Northeast Trade winds (Lázaro et al., 2005) along with the NECC strengthening are responsible for fact that the MC roughly reaches the 20° N parallel, just south of Cap Blanc. This process is associated with the cessation of upwelling and the Canary Current (CC) in this place (Mittelstaedt, 1991; Stramma et al., 2008).

3.2 Mid-depth ocean

Intermediate waters, namely, Antarctic Intermediate Water (AAIW) and Upper Circumpolar Water (UCPW) cross the equator northward mainly in the Western Atlantic between 500 m and 1200 m depth (Oudot et al., 1999). The vertical minimum of potential temperature (Reid, 1997) and more so the intermediate maximum of silicate concentrations (Oudot et al., 1999) are distinguishing features of UCPW in the equatorial zone. AAIW is carried by several interchanging eastward and westward flowing currents in the equator area (Stramma and Schott, 1999; Brandt et al., 2006). Extended horizontal oxygen minimum zones (OMZs) exist in the eastern tropical Atlantic between 200 and 800 m due to microbial respiration of the ~~excessive~~ large amounts of organic matter from the nearby North African upwelling area and weak water ventilation (Karstensen et al., 2008). ~~Extended horizontal OMZs exist in the eastern tropical Atlantic between 200 and 800 m.~~ The core of the North Atlantic OMZ include SACW and AAIW layers (Stramma et al., 2005). The major pathways to the northern OMZ are subsurface eastward jet currents located south of 10° N: the NICC at 2° N, the NEUC at 4° N, and the northern branch of the NECC at 8–9° N (Stramma et al., 2005; Karstensen et al., 2008; Brandt et al., 2010), while the core of the northern OMZ lies further north. The link between these subsurface jet currents and the OMZ is formed simultaneously by the cyclonic circulation around the GD, a general uplift of the isopycnals within the surface and subsurface levels (Siedler et al., 1992; Lázaro et al., 2005).

3.3 Deep ocean

North Atlantic Deep Water (NADW) is formed in the North Atlantic by convection and mixing and transported southward. NADW penetrates into the Equatorial Atlantic at depths almost similar to the Deep Western Boundary Current (DWBC), and bifurcates into an eastward and southward flow, correspondently into the open ocean and along the western boundary (McCartney, 1993). According to Wüst (1935), upper NADW (UNADW) can be recognized by the mid-depth salinity maximum (~~1500–2000~~ 1500–2000 m deep), while middle NADW (MNADW) at 2000–2500 m deep and 3700 m deep lower NADW (LNADW) are recognized by the oxygen maxima. In ~~the~~ Molinari et al. (1992), waters that had been recently ventilated are described as having had contact with the atmosphere either directly or indirectly by mixing on the time scale of the measurable transient tracer — chlorofluorocarbon (CFC). The maximum of one of the CFCs (F11 — trichlorofluoromethane) represents LNADW (Rhein et al., 1998).

Two cores of recently ventilated (with higher levels of F11) NADW from the northern hemisphere are advected along the boundary and east to the Mid-Atlantic Ridge (MAR) ~~(Molinari et al., 1992)~~Molinari et al. (1992). A DWBC shallow core is

centered centred at about 1500 m and a deeper one — at about 3500 m. The upper core of high F11 content, limited by the 3.2 and 4.7°C potential temperature isotherms, is typically associated with the deeper core, which is limited by the 1.8 and 2.4°C isotherms. The Ceara Rise blocks the flow of the DWBC waters with potential temperature below 1.8°C to the equator, causing it to recirculate back to the north.

More dense Denser Antarctic Bottom Water (AABW) flows northwars northwards though Atlantic Ocean basins and generally lays underneath lies beneath NADW at the bottom. The velocity field of AABW (water with σ_4 °4 > 45.90 kg m^{-3}) is influenced by the overlying DWBC (Rhein et al., 1998). The AABW consists of old deep-water masses (Reid, 1994) (Reid, 1994) with negligible F11 concentrations. According to Rhein et al. (1998), AABW bifurcates at the equator: roughly 30 % percent of the northward AABW flow comes to the Guiana Basin through the Equatorial Channel at 35° W. The A large proportion of AABW turns east to through the Romanche Fracture Zone and to the Eastern Atlanticwith a possibility of , with a possible recirculation in the Brazil Basin. The sloping topography of Guiana Basin as well as the limitation of the AABW upper boundary by the strong eastward flowing NADW cause the fact that the northward directed geostrophic flow of AABW is to be most pronounced only to the east from of the Ceara Rise. Passing the Ceara Rise, AABW flows to the Guiana Basin central part central part of Guiana Basin. The high level of F11 (> 0.07 pmol kg$_{-1}$) from LNADW affects the closest to it AABW part — the one nearby the part of AABW closest to the Ceara Rise, thus this AABW branch also experiences a rise in F11 content in comparison with the far eastern AABW branch. To the north from the Ceara Rise similar conditions are found its far eastern branch. Similar conditions are found to the north of Ceara Rise (Rhein et al., 1998). According to (Whitehead Jr and Worthington, 1982; Rhein et al., 1998)Whitehead Jr and Worthington (1982) and Rhein et al. (1998), the core of AABW is located to the east the of Ceara Rise at 43.3° W.

AABW mixes with LNADW in the fracture zones at equator, so AABW in the Eastern Atlantic differs from the similar water in the Western Atlantic (Rhein et al., 1998). There are two important features for the Eastern Equatorial Atlantic (McCartney et al., 1991). First, the potential flow of AABW through the Kane Gap from the Sierra Leone Basin to the Gambia Abyssal Plain and back . Secondand second, the potential AABW flow through the Vema Fracture Zone.

According to Arhan et al. (1998) the eastward transport of NADW along the equator is weak, but nevertheless plays a leading role for the maintenance of the equatorial tongue of UNADW. Even though the eastward mean velocities are weak in the equatorial tongues of NADW, the question is of the ultimate fate of this flow as it reaches the African continental slope. There are two cyclonic flows in the deep layers of Eastern Atlantic, associated with NADW — the Gambia Basin one and the Sierra Leone Basin.

4 Results and discussion

4.1 SPM concentration

The distribution of SPM within the Ioffe-2000 transect is presented in Figure 3, while background hydrophysical and hydrochemical conditions were described in detail in (Sarafanov et al., 2007). The obtained Sarafanov et al. (2007). The measured volume SPM concentrations varied from 0.01 to 0.40 ppm within the Ioffe-2000 transect and up to 4.1 ppm at the stations at the

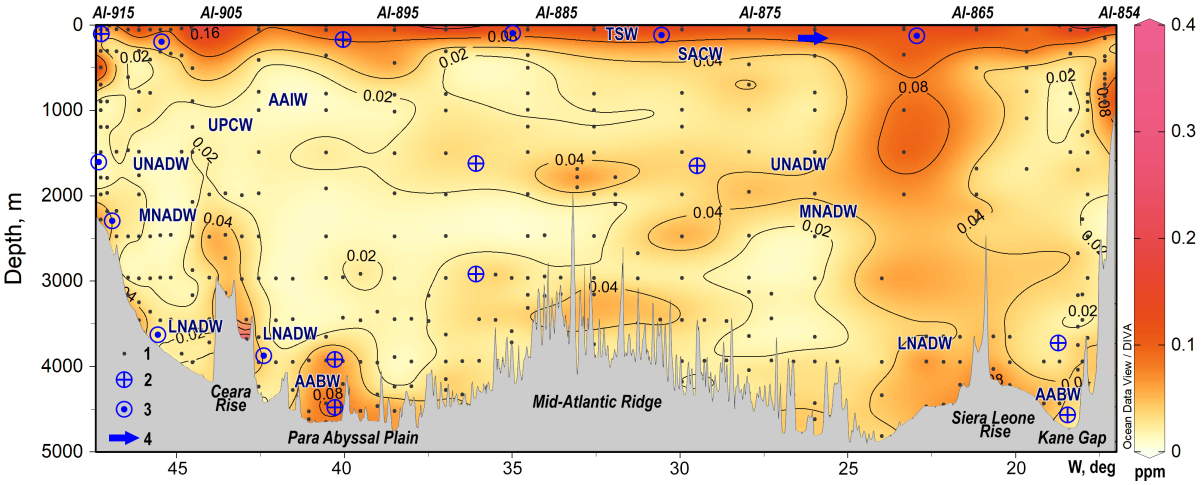

Figure 3. Distribution of the SPM volume concentration (ppm) on the Ioffe-2000 transect, done with Ocean Data View (Schlitzer, 2018). 1 — sampling points, 2 — northward current, 3 — southward current, 4 — eastward current. Isolines are in geometric progression, for water mass abbreviations see text. Bottom topography from Sokov et al. (2002) The interpolation was done via the DIVA gridding (Barth et al., 2010) with 25 permille X-scale length and 65 permille Y-scale length.

Northwest African upwelling area. The work of McCave (1983) contains both the partly comparable dataset of SPM volume concentrations with a slightly wider size range (1.26–32 μm), and the apparent particle densities, that lies between 1.65 and 2.23 mg mm$_{-3}$. Applying these apparent densities to our volume SPM concentrations, we got the implied weight concentrations about 0.016 to 0.35 mg L$_{-1}$ (up to 0.8 mg L$_{-1}$ in exceptional circumstances), which agrees with Brewer et al. (1976) and Gardner et al. (1985a).

4.1.1 Upper ocean

In the upper layers, most commonly, the vertical distribution of SPM has a surface maximum caused by primary production, decreasing exponentially towards the deep. The main reason for this is the fact that the upper ocean ~~contain~~ contains both the external SPM sources (river discharge, atmospheric input) and the internal SPM sources (primary production) (Chester, 1990). Another reason for particle accumulation in the surface layer may be the pycnocline, which slows the sedimentation (Emelyanov, 2005). The "sedimentation barrier"" was presented by a visible pycnocline at depths of 50–150 m to the west of the 30° W and ~~0–100~~ 0–100 m to the east of this point on the Ioffe-2000 transect (Sarafanov et al., 2007). It was shown for the Eastern Equatorial Atlantic that the largest particulate elemental and mass concentration gradient occurs at the base of the mixed layer, where the particle and organism maximums are located. The source of the vast majority of particles in the upper open ocean waters is internal and ~~is~~ consists basically of particulate organic matter (POM), ~~CaCO$_3$~~CaCO3, and biogenic silica. A large proportion of the POM produced in surface waters is regenerated in the euphotic zone. Although the net transport

of organic matter ~~have~~ has to be downward to fuel the lower layers of the water column, there is also an upward component to transport. Positively buoyant particles, including lipid-rich eggs, larvae and, possibly, carcasses of deep-sea animals are examples of particles which undergo upward transport (Smith et al., 1989).

~~Distribution of the SPM volume concentration (ppm) on the Ioffe-2000 transect, done with (Schlitzer, 2018). 1 — sampling points, 2 — northward current, 3 — southward current, 4 — eastward current. Isolines are in geometric progression, water masses abbreviations see in text. Bottom topography from Sokov et al. (2002)~~

The Ioffe-2000 transect did not reach the SPM-rich ~~coastal~~ shelf waters, yet the coastal SPM source has caused a local SPM maximum at the margins of the transect at a depth of ~~400–800~~ 300–900 m (up to 0.18 ppm ~~).~~ in the west and up to 0.09 ppm in the east). The eastern edge of the Ioffe-2000 transect is located above the gentle slope between 200 m and 2000 m named Guinea Marginal Plateau (Egloff, 1972), adjacent to the high productive Guinea shelf (Vladimirov et al., 1990; Burlakova et al., 1997). Strong currents (Mittelstaedt, 1991; Stramma et al., 2005, 2008) and implied internal wave activity, based on significant density gradients on the shelf (0–200 m) (Sarafanov et al., 2007), may provide a framework for the SPM lateral transport from the shelf along the gentle Plateau slope. It was the Amazon River that caused the ~~far more pronounced influence of the American coast in comparison with the African one~~more pronounced rise in SPM concentration at the western edge of transect. It is well known that the surface SPM transport from the Amazon River to the open ocean turns to the ~~north-east~~ northeast alongside the coast (Gibbs, 1974). According to Sarafanov et al. (2007), the warm, high-saline and silicate-poor upper waters observed on the Ioffe-2000 transect above 400–500 m were advected mostly by the NBC. The NBC core was located immediately westward of the studied transect near the shelf break (Johns et al., 1998). A signature of the NBC eastern periphery is located between 46° W and 47° W at depths of 150–500 m (Sarafanov et al., 2007). The SMP concentrations within the NBC are relatively low (stations AI-910–AI-912). The main evidence of the SPM supply from the Amazon River to the shelf and the continental slope is a huge sediment body — the Amazon Cone. Bottom SPM maxima of Amazon River origin are able to form INL falling from the shelf break. INLs are mostly caused by the detachment of BNLs over the breaks in the slope (McCave et al., 2001). One of the INLs was apparently observed during the Ioffe-2000 transect as a significant rise in the SPM concentration below the NBC.

Sarafanov et al. (2007) shows the NEUC equatorward pathway at 44–46° W. We have suggested that such V-shaped isopycnals at 46° W between the NBC and NEUC (Sarafanov et al., 2007, Fig. 3A) correspond with the aforementioned large eddy-like feature, the semi-permanent “Amazon Eddy” (Bruce et al., 1985).

The northern branch of the SEC (nSEC) is associated with the northwestward or northward near-surface flow at 38–41° W, which recirculates northward into the NECC. Probably, the local surface maximum of the SPM concentration at 44° W was caused by the nSEC and NECC convergence. The surface SPM maximum was also noted in the most intense cross-transectal flow of the NECC at 35–37° W (Sarafanov et al., 2007).

The eastward rise of the isopycnals at 28–25° W and their deepening at 24.5–21.5° W at 150–500 m ~~indicate~~ indicates the southern periphery of the GD on the Ioffe-2000 transect ~~(Sarafanov et al., 2007)~~(Sarafanov et al., 2007, fig.3A). Immediately east of the GD (21.5–18° W) the S-shaped double rotation (a combination of the cyclonic and anticyclonic structures) of the NEUC ~~(Stramma et al., 2008, fig. 12) occered~~(Stramma et al., 2008, fig.12) occurred. It is known that the GD influences biological ~~activities~~activity, so the chlorophyll-a concentration is high in this region and linked to the intensity of the doming

(Signorini et al., 1999; Pradhan et al., 2006; Doi et al., 2009). ~~So the~~ The local SPM maximum ~~in~~ below the GD area within the Ioffe-2000 transect ~~correlate~~ agrees with this data. Overall, the SPM distribution within the Ioffe-2000 transect's upper layer mainly reflects surface circulation patterns (Biscaye and Eittreim, 1977) as well as particle transport (vertical and horizontal).

4.1.2 Mid-depth ocean

According toSarafanov et al. (2007), the intermediate waters on the Ioffe-2000 transect were recorded as an area of low in ~~salininty~~ salinity and rich in silicate waters, which extends at depths of ~~–~~400–1200 m. The AAIW main entrance to the Northern Hemisphere is located in the western part of the transect (west of 36° W). Both AAIW and UCPW do not come along the Brazilian slope while flowing from the western equatorial basin to the tropical North Atlantic, but rather flow in the interior ocean.

Usually the intermediate waters correspond with the upper part of the clear water minimum. Clear water is referred to the minimum in the SPM concentration that is commonly located at ~~varyious~~ various mid-depths ~~(Biscaye and Eittreim, 1977)~~(Eittreim and Ew Concentrations of the SPM within this layer are 10–100 times lower than in the upper ocean but still reflect, in general, a similar geographic distribution with high values in the coastal zone and the lowest values at the open ocean. As was mentioned above, the clear water layer SPM concentration reflect, also, the lateral supply of the SPM from the coastal areas (Biscaye and Eittreim, 1977). However, the intermediate waters on the Ioffe-2000 transect were not influenced by the lateral source too strongly, so the SPM concentrations were low (0.01–0.03 ppm).

On the contrary, the wide area below the GD (~~19–25~~19–25° W) is noteworthy due to extremely high SPM concentration for this clear water layer~~SPM concentration~~, which primarily reflects the pattern of productivity in the upper waters (Eittreim et al., 1976). We suggest that this SPM-rich area was caused by the extra high bioproductivity levels within the Northwest African upwelling and, probably, the GD area (Fig. 4). Equatorward transport of the POM is carried out by the interaction of the CC and the aforementioned system of equatorial currents. Additional explanation for the POM supply is the low dissolved oxygen ~~levels~~ level (OMZ signature), that was observed at 300 to 700 m depth about 20–25° W and further westward to the MAR ~~(Sokov et al., 2002)~~(Sokov et al., 2002). Not only is the oxygen minimum caused by the POM supply, but it also prevents organic particles from destruction.

4.1.3 Deep ocean

It is known that the vertical and zonal structure of the deep and bottom waters, i.e. NADW and AABW, in the Eastern Atlantic are significantly more homogeneous than in the Western Atlantic. The Eastern Atlantic generally shows low turbidity (SPM concentration) levels within the NADW and AABW in comparison with the Western Atlantic (Eittreim et al., 1976). The water exchange in the deep layers of Eastern Atlantic is almost negligible in comparison with the intense northward flow of AABW to the east of the Ceara Rise in the western basin, that was noted during the Ioffe-2000 transect (Sarafanov et al., 2007).

The Eastern Atlantic. The research to the east of MAR at the Ioffe-2000 transect allowed us to note two peculiarities. The first one was the northward NADW flow through the Kane Gap into the Gambia Basin, while the second one pointed out the dominance of LNADW in the near-bottom layer west of the Sierra Leone Rise.

The deep waters correspond with the lower part of the clear water minimum. However, ~~the abnormally high~~ abnormally high SPM concentrations for these depths ~~SPM concentrations~~ were noted above the Sierra Leone Rise. This SPM concentration anomaly was connected with another ~~one above~~ above it in the mid-depth ocean. There ~~are also~~ is also a slight horizontal "tail~~"~~" with increased SPM concentration spreading almost to the MAR. The probable reason for ~~"tail" existence~~ existence of the "tail" is the cyclonic flow over the Gambia Abyssal Plain (Arhan et al., 1998). We propose to explain this "vertical anomaly~~"~~" by using the ballast hypothesis (Armstrong et al., 2001; Louis et al., 2017), which is based on the correlation between the fluxes of particulate organic carbon (POC) and minerals in the deep ocean. ~~Accordinc~~ According to hypothesis description in Van der Jagt et al. (2018), biogenic aggregates are ballasted with biogenic and lithogenic minerals, so their sinking velocities increase. Minerals start to get attached to aggregates both in the surface layer and deeper: during the aggregates formation or when aggregates "scavenge~~"~~" mineral particles while sinking. The fact that ballasted aggregates sink with higher speed is the main reason for them to be remineralized at a greater depth in comparison with non-ballasted aggregates. ~~Differect~~ Different aggregates are incorporated with different number of minerals due to different stickiness, which is controlled by the amount of transparent exopolymer particles (TEP) (Alldredge et al., 1993). TEP-precursors are produced mainly by phytoplankton (Passow and Alldredge, 1994). The amount of TEP in the ocean is huge, they ~~occure~~ occur as "sticky~~"~~" gels (Passow, 2002), so TEP act as a glue matrix for other solid particles (i.e., detritus), forming larger aggregates ("marine snow~~"~~") and playing a crucial role in the carbon export from the surface to the deep ocean (Passow et al., 2001).

The SPM in regions with high external supply (for example, the North Atlantic) with their high ~~dust sedimentary~~ sedimentary dust inputs consists mostly of lithogenic material. For instance, the surface waters off Cap Blanc (Iversen and Ploug, 2010) and GD (Bubnova et al., 2020) are exposed to the Saharan dust. The Saharan dust deposition may cause the abiotic formation of TEP, which results in the aggregates formation and enhancing the POC export (Louis et al., 2017). Dust is able to ballast into marine snow aggregates (and fecal pellets) ~~ans~~ and it also increases the oceanic primary production due to input of dust-related micronutrients (Van der Jagt et al., 2018). Potential strength of the so-called ~~"~~"lithogenic carbon pump~~"~~" (Bressac et al., 2014) potentially depends on the physical and chemical TEP-precursors featured, which, in turn, stand on the composition and physiological state of the phytoplankton community. The Northwest Africa offshore zone shows high levels of primary production and SPM concentrations (Fig. 4). This area is also exposed to ~~the Saharan dust abundance. The excessive~~ abundant Saharan dust input. The resulting large number of ballasted aggregates is ~~lately~~ then transported equatorward via the CC and consistent flow of the NEC, NECC and GD (equatorial currents system), reaching the Ioffe-2000 transect area.

The Van der Jagt et al. (2018) study showed that the total volume of aggregates increased ten times due to dust deposition, while size-specific sinking velocities of the dust-ballasted aggregates ~~incresed~~ increased two times. It was also shown that the dust-ballasted aggregates carried only 50 percent of the volumetric POC amount in comparison with non-ballasted aggregates. Thus, the overall POC flux driven by dust deposition may rise up to ten times due to the abundance of aggregates. As we remember, fast sinking aggregates are remineralized deeper leading to an increase in the POC fluxes to the deep sea layers (Van der Jagt et al., 2018), which preserves the high SPM concentrations down to the deep ocean. Such fast sinking ballasted aggregates, which were transported from the Northwest Africa upwelling area, caused the abnormally high SPM concentrations above the Sierra ~~leone Rise within~~ Leone Rise in the Ioffe-2000 transect.

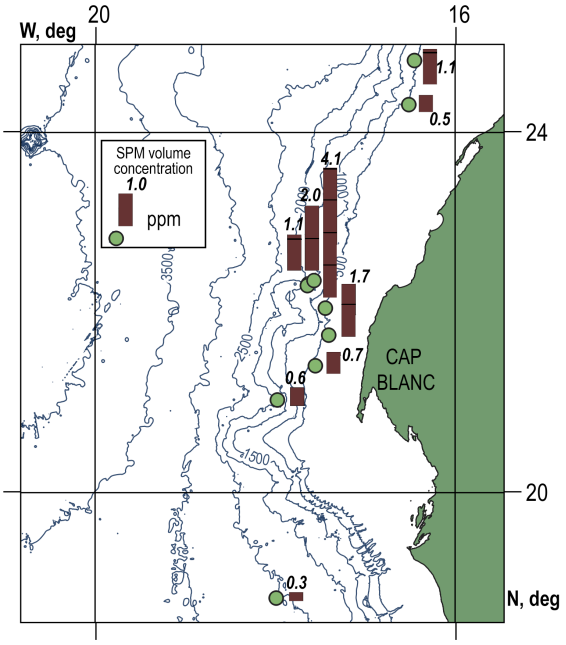

Figure 4. ~~The schematic~~ Schematic distribution of surface SPM concentrations (ppm) ~~at~~ in the ~~Nortwest Africa~~ Northwest African upwelling area prior to the Ioffe-2000 transect. Isobaths every 500 m.

The Western Atlantic. The vast area to the west of the MAR within the Ioffe-2000 transect experiences an increase in the SPM concentrations, caused by DWBC. It is well-known that there are two reasons for the bottom currents to maintain high loads of SPM: potential resuspension and, far more importantly, selective deposition. The SPM may be transported far within the BNLs, as was shown for clay minerals (Petschick et al., 1996). The most intense BNLs in the western Atlantic are found in the southwestern Argentine Basin and northern North American Basin; while the lowest bottom water turbidity is located in the equatorial regions (Eittreim et al., 1976; Biscaye and Eittreim, 1977). Nevertheless, bottom SPM concentrations west of the MAR are still higher in comparison with the eastern part of the Equatorial Atlantic. According to Sarafanov et al. (2007), the southward boundary flow of UNADW was traced in the western basin along the continental slope at the depths of 1400–1500 m. MNADW southward flow was noted at 1900–2600 m with the 100 km wide recirculation. The general LNADW flow was noted at 3700 m depth. The deep cyclonic cell in the Guiana basin (McCartney, 1993; Arhan et al., 1998) at NADW depth near the Ceara Rise western slope and west of the MAR between 42° W and 36–37° W. This northward recirculation of LNADW joins the northward flow of AABW.

The noticeable BNL ~~within~~ in the western basin is located at 1900–2600 m above the American slope (the Amazon Cone). We suggest that the main reason for its ~~occurence~~ occurrence is the interaction between the shallow core of the DWBC and the Amazon River solid load.

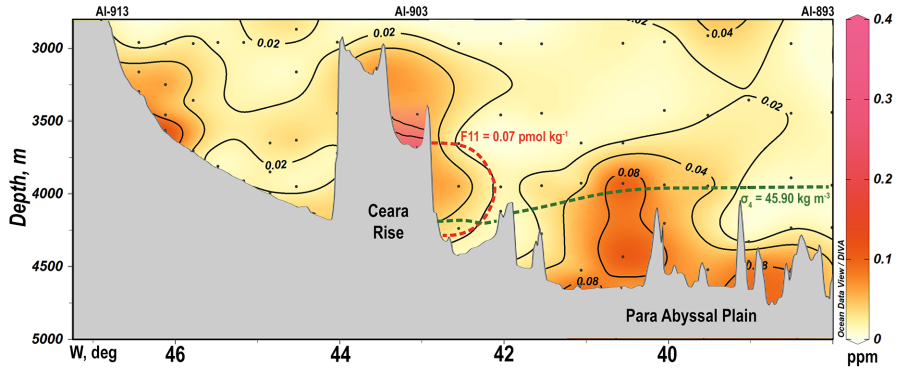

Figure 5. The SPM volume concentration at the western part of the Ioffe-2000 transect: green dashed line — the upper boundary of AABW; red dashed line — the DWBC boundary, based on the F11 (after Rhein et al. (1998), 4.5° N transect). Isolines in geometric progression.

The weak INL deepening from the slope to the east was noted at a depth of 3200–3700 m (Fig. 5). It is enhancing above the Ceara Rise as a result of the DWBC ~~intencification~~ intensification due to the interaction with bottom topography. This INL can be traced to the east from the Ceara Rise (4300 m ~~depthe~~ depth and 42.5° W), where the deep DWBC core is marked by high F11 level.

~~This~~ The main reason for the SPM concentration rise at the depth of 3500–4300 m between 41.5° W and 39° W with the peak at 40.5° W is the northward recirculation of SPM-rich LNADW.

The general northward pathway of AABW (σ_4 ~~°~~4 > 45.90 kg m^{-3}) ~~within~~ across the Ioffe-2000 transect is located in the Para Abyssal Plain bottom layer. AABW core was found in the 40–42° W troughs, flowing along the Ceara Rise eastern slope (Sarafanov et al., 2007). Studies (Whitehead Jr and Worthington, 1982; Rhein et al., 1998) show the AABW core to be separated from the bottom and located at a depth of 4400–4500 m. AABW has high SPM concentrations in comparison with the clear water layer, mostly in the 40–41° W troughs. The SPM concentration maximum within AABW (Fig. 5) is aligned with the AABW core separated from the bottom ~~AABW core~~ (4400–4500 m). The reason for the separation may be the bottom rise ("dam~~"~~"), which is located up-stream AABW flow (Whitehead Jr and Worthington, 1982). The "dam~~"~~ " blocks the lower part of AABW flow and coinciding BNL at the depth of 4500 m, ~~creatint~~ creating the INL from BNL. One of the most notable similar nephelometric features was described for the Puerto Rico Trench near the Navidad sill (Tucholke and Eittreim, 1974). The BNL to the east ~~from~~ of the AABW flow core is likely caused by AABW southward recirculation (Sarafanov et al., 2007).

The extremely high SPM concentration (0.36 ppm) was noted in bottom layer above the Ceara Rise (AI-903, depth 3678 m, 18 m.a.b.). The potential reason for that may be interaction between the SPM-rich DWBC and a local feature in the bottom topography. Figure 6 shows, that AI-903 station was conducted near the terrace ~~brake~~ break (3800 m). The terrace slope is low-angle (0.7°), while below the terrace ~~brake lays~~ break lies a far steeper (3.1°) slope (3800–4300 m). This 15-km wide area with the ~~incline drop perturbs the DWBC core homogenety: the current part~~ steep incline perturbs the homogeneity of the DWBC core: the part of the current above the flat terrace slows down, while the steeper slope ~~suggests~~ causes a higher bottom current speed (Bowden, 1960). The current ~~slowing~~ slow-down above the terrace is able to cause an eddy. The V-shaped terrace

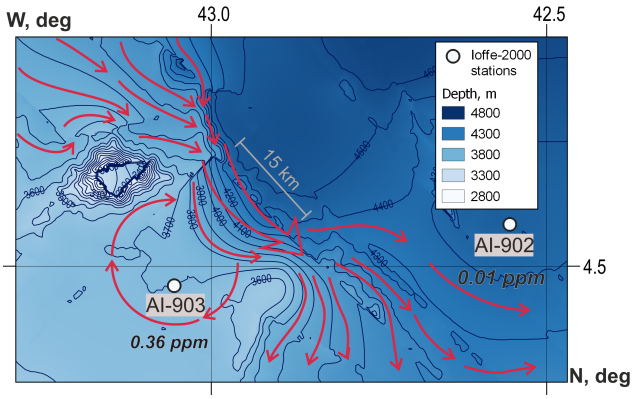

Figure 6. The Ceara Rise SPM maximum: bottom topography (GEBCO Bathymetric Compilation Group, 2020) and the DWBC (red lines).

(see 3700 m isobath) allows ~~to assume~~ the assumption that this eddy is the ~~trapped topography~~ topographically trapped one. The eddy ~~originated~~ originating from the SPM-rich DWBC causes an additional SPM concentration boost near the bottom. The proposed hypothesis undoubtedly needs to be confirmed by additional research.

The MAR area. High levels of the SPM concentration were also noted above the MAR. ~~The~~ There is the northward recirculation of rich in the SPM NADW (Sarafanov et al., 2007), which was noted both sides of the MAR at 36–40° W and 29–32° W. Another type of currents in the area is tidal currents (Morozov, 2018). According to Lavelle (2012), both these currents may be accelerated along the flanks of the ridge and represent a significant stirring mechanism for abyssal flow and cause the SPM concentration rise. Moreover, the axial region of the MAR including the rift zone experiences high seismicity and bears a ~~big~~ large number of earthquake ~~epicenters~~ epicentres as well as the sulfide mineralization zones of various origins and bedrock zones showing strong hydrothermal imprints (Mazarovich and Sokolov, 2002); in particular in the Sierra Leone fracture zone, i.e. immediately below the Ioffe-2000 transect (see Fig. 1). Both high seismicity and strong hydrothermal activity may also be able to cause increased SPM concentrations in the bottom layer. ~~These factors coincide with tidal currents (Morozov, 2018), potentially causing the INL and BNL above the MAR. The relatively high SMP concentrations above the MAR may be also caused by the northward recirculation of NADW (Sarafanov et al., 2007) rich in the SPM, which was noted both sides of the MAR at 36–40° W and 29–32° W.~~

4.2 Grain-size of the SPM

The size distribution of suspended particles is generally considered to be a function of the source and nature of the particles, processes of aggregation and the "age~~"~~" of the suspension ~~(McCave, 1985)~~(McCave, 1983, 1985). SPM grain sizes in cumulative number distribution from Ioffe-2000 transect follow a hyperbolic Junge distribution with slopes between ~~–2.6 and –4.2~~–1.9 and –3.7 (Fig. 7), which correspond with (McCave, 1975), where slopes were mainly between –2.4 and –3.6. The difference ~~occures~~ occurs due to the fact that (McCave, 1975) had ~~wider size spectum~~a wider size spectrum. The overall cumulative

number distribution for Ioffe-2000 transect were recorded as a wavy line with an overall slope approximating ~~–3.4~~ –2.7 which is similar to (McCave, 1984, 1986; Nowell et al., 1985).

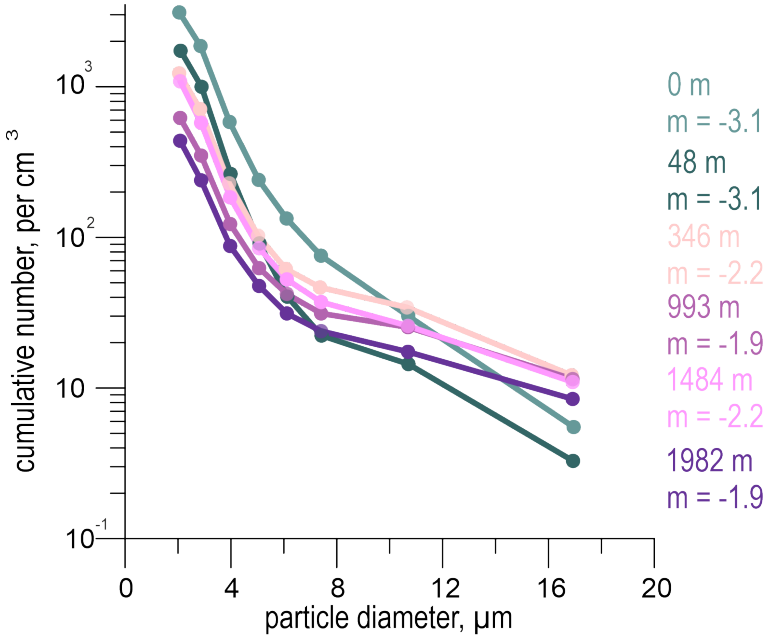

Figure 7. Cumulative particle number distribution for AI-868 station showing both "old" suspension in the upper ocean with the slope of the distributions close to –3 and "fresh" in the water column with steep slopes about –2. Station AI-868 is a part of the SPM-rich "vertical anomaly". X-axis is particle diameter, Y-axis is cumulative particle number in log10 scale.

The explanation for volume-size distributions was generally based on the results of the HEBBLE project in abyssal waters (the Nova Scotia Rise, ~~1977–1984~~1977–1984) (McCave, 1983; Nowell et al., 1985; McCave, 1985). The sizes measured by a Coulter Counter in this project mainly showed the bimodal structure with a fine mode between 2 and 10 µm and a coarse mode between 20 and 60 µm.

Due to the aperture-tube truncation of 70 µm of the Coulter Counter during the Ioffe-2000 cruise there was a possibility to count the fine part of the coarse mode only. The volume-size distributions display: a) an increased proportion of the 7–21 µm fraction, suggesting the coarse mode, b) a subsidiary fine-mode with the peak size ranges about 2–4 µm, and c) an intermediate mode at 8–13 µm, that was not mentioned in the HEBBLE project.

The most representative volume-size distributions in our study are shown in Figure ~~7.~~ 8. According to McCave (1983, 1984), there are two most effective physical mechanisms for changing the size distributions: aggregation of small particles (below 1.5–8 µm) by Brownian motion and collection of smaller particles by turbulent agitation with larger particles. Thus, the fine mode mainly consists of aggregates. The more turbid suspensions according to ~~(Gardner et al., 1985b)~~ Gardner et al. (1985b) contain a coarser fine mode (~ 8 µm) than the lower concentration suspensions with a mode of 2–3 µm. According to ~~(McCave, 1984)~~McCave (1984 oceanic particle size volume distribution shows pronounced peaks in BNLs with active resuspension and in surface waters with

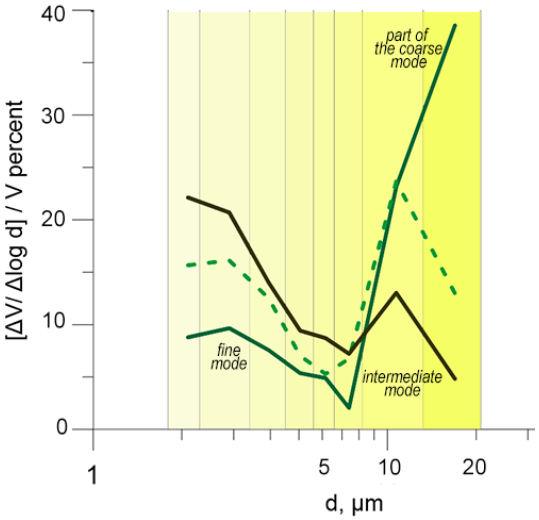

Figure 8. The typical examples of the bimodal volume-size SPM distribution. X-axis is particle diameter, Y-axis is probability density function. Green solid line — dominance of coarse TEP (station AI-898, 3927 m); dashed green line — intermediate mode, caused mostly by phytoplankton, detritus and TEP (station AI-875, 54 m); solid brown line — distribution, potentially caused by the weakened TEP-mode (AI-859, 4732 m). Size intervals are marked with color and thin vertical lines.

active primary production. The aggregation rate of 1.5–8 μm particles in the upper ocean depends on filtration by zooplankton. The fine mode, which is weakly pronounced in our data, is explained by a relatively low ~~concentrations~~ concentration (up to 0.36 ppm).

The upper ocean is the area, where the particle production and modification of the initial size distributions occurs ~~most turbulently~~controlled by turbulence. Increased shear in pycnoclines and ~~large Brunt-Vaisala frequency generally results in~~ internal wave-driven turbulence would promote aggregation and lead to a further smoothing of the size distribution (equivalent to a cumulative particle number distribution with a slope of ~~-3~~ –3) of SPM (McCave, 1984). The horizontal supply of SPM to the mid-water in the open ocean is relatively slow, therefore, a part of fine material in SPM is old (years old), so the size distribution should not have significant peaks. The flat size distributions are best explained by the sub-equal production of particles of different ~~sized~~sizes. The coarse mode (20–60 μm), according to McCave (1985), is a result of aggregation, where a significant role is played by mucus. Lately, as was mentioned above in the paper, mucus has started to be referred as TEP. There are no strong vertical gradients of mucus concentration suggesting a bottom source, so it is presumed that the material results from surface productivity and has settled rapidly. This viewpoint is supported in ~~(Emery and Honjo, 1979)~~Emery and Honjo (1979), where the same type of material from surface waters is described and called an "(organic) film~~"~~". It was shown that the film is most abundant in upwelling areas. The intermediate mode (8–13 μm) was dominant in the surface waters (50 m depth) in

the samples with high SPM levels (~~.3~~ 0.3 ppm). Its occurrence is supposedly caused by high concentration of phytoplankton with cell size less than 10 μm, as well as newborn TEP and detritus. The vertical distribution of different fraction sizes of phytoplankton in the euphotic zone of the Equatorial Atlantic shows that the dominant plankton cell size at the 50 m depth is 3–20 μm (11.5 μm on average) (Herbland et al., 1985). This intermediate mode could not be revealed during the HEBBLE project, because the project was aimed exclusively at abyssal waters.

5 Conclusions

The Ioffe-2000 transect presented a "screenshot~~"~~ " of volume SPM distribution in the northern part of the Equatorial Atlantic against the background of hydrographic data. Alongside the general agreement with the three-layer model of the ocean SPM distribution, there were some large regional non-uniformities of SPM concentrations and grain size. The international studies of last two decades allowed us to explain those non-uniformities:

1. The most noticeable anomaly is a wide area of high SPM concentrations above the Sierra Leone Rise spreaded from the upper ocean, through the intermediate layer of clear water and down to the ocean bottom. We suggest that this "vertical anomaly~~" was~~ " originated from the Northwest African upwelling area, where the aggregation process exists, since the plankton exposed to ~~the Saharan dust abundance form a big~~ abundant Saharan dust form a large number of ballasted aggregates. The aggregates were lately transported equatorward via the CC and equatorial currents system (including the GD). Our ~~study results agrees~~ studies results agree with the fact that higher ~~aggregates~~ aggregate numbers and higher sinking velocities may increase the carbon export to deep ocean layers. Changes in dust sedimentation may bring about drastic changes in the global ocean due to the boost that trace nutrients from dust may ~~do~~ cause for primary production.

2. Deep and bottom waters of the western part of the Equatorial Atlantic show increased levels of the SPM concentrations. The INL deepening from the American slope to the east was noted at ~~the depth~~ depths of 3200–3700 m. The high SPM concentrations in the bottom layer above the Ceara Rise is caused by the interaction between the SPM-rich DWBC and a local feature of bottom topography. AABW has ~~incresed~~ increased SPM concentrations mostly in the 40–41° W troughs. The SPM maximum is located in the AABW core (4400–4500 m), separated from the bottom. The explanation for this may be that the bottom rise located up-stream ~~current~~ serves as a "dam~~""~~", blocking the lower part of AABW flow and ~~coinciding~~ its BNL.

3. The sizes of suspended particles in the cumulative number distribution follow a hyperbolic Junge distribution with slopes between ~~–2.6 and –4.2~~ –1.9 and –3.7; the averaged slope was approximated as ~~–3.4~~ –2.7, which fits into the general understanding.

The volume-size distributions displayed two ~~HEBBLE-comparable modes~~ modes -comparable to those found in HEBBLE: a fine-mode 2–4 μm and an increased proportion of the 7–21 μm fraction, suggesting the coarse mode (20–60 μm). There was an additional intermediate mode 8–13 μm. It is well known, that the fine mode is mainly represented by aggregates formed from small particles by Brownian motion. The weakly pronounced fine mode could be suggesting a relatively old age of SPM and low concentrations. The coarse particles (7–21 μm) likely represent aggregates with biogenic mucus (TEP), which plays a

significant role in particle aggregation. ~~Additional~~ The additional intermediate mode (8–13 μm) is dominant in the SPM-rich surface waters and is presumable the result of phytoplankton growth and the initial TEP formation.

Data availability. The coordinates (Lat, Lon) of the Ioffe-2000 sampling stations, depths of samplings and volume suspended particulate matter concentrations are given in Supplement 1.

Author contributions. Vadim Sivkov: conceptualization, formal analysis, investigation, resources, supervision, funding acquisition; Bubnova Ekaterina: methodology, data curation, visualization, formal analysis. All authors have read and agreed to the published version of the manuscript.

Competing interests. The authors declare no conflict of interest. The funders had no role in the design of the study; in the collection, analyses, or interpretation of data; in the writing of the manuscript, or in the decision to publish the results.

Acknowledgements. The preliminary data processing and surface ocean data interpretation were conducted with financial support of the state assignment of IO RAS (Theme ~~0128-2021-0012~~0128-2021-0016), the data interpretation and conclusions regarding the modern AABW circulation was supported by Russian Science Foundation (project 19-17-00246). The article was finished in kind memory of academician A.P. Lisitsyn (IO RAS) who helped with this research~~enormously~~. Marina Ulyanova and Leyla Bashirova contributed with valuable ~~advices~~ advice and the fruitful discussions. Authors also would like to thank Professor Ian Nicholas McCave, who definitely made us to improve the paper significantly.

References

Alldredge, A. L., Passow, U., and Logan, B. E.: The abundance and significance of a class of large, transparent organic particles in the ocean, Deep Sea Research Part I: Oceanographic Research Papers, 40, 1131–1140, https://doi.org/10.1016/0967-0637(93)90129-Q, 1993.

Arhan, M., Mercier, H., Bourles, B., and Gouriou, Y.: Hydrographic sections across the Atlantic at 7°30N and 4°30S, Deep-Sea Research I, 45, 829–872, 1998.

Armi, L.: Mixing in the deep ocean: the importance of boundaries., Oceanus, 1978.

Armstrong, R. A., Lee, C., Hedges, J. I., Honjo, S., and Wakeham, S. G.: A new, mechanistic model for organic carbon fluxes in the ocean based on the quantitative association of POC with ballast minerals, Deep Sea Research Part II: Topical Studies in Oceanography, 49, 219–236, https://doi.org/10.1016/S0967-0645(01)00101-1, 2001.

Barth, A., Alvera-Azcárate, A., Troupin, C., Ouberdous, M., and Beckers, J.-M.: A web interface for griding arbitrarily distributed in situ data based on Data-Interpolating Variational Analysis (DIVA), Advances in Geosciences, 28, 29–37, 2010.

Biscaye, P. E. and Eittreim, S. L.: Suspended particulate loads and transports in the nepheloid layer of the abyssal Atlantic Ocean, Marine Geology, 23, 155–172, https://doi.org/10.1016/0025-3227(77)90087-1, 1977.

Bischof, B., Mariano, A. J., and Ryan, E. H.: The North Brazil Current, https://oceancurrents.rsmas.miami.edu/atlantic/north-brazil.html/, online; accessed 20-November-2020, 2003.

Bourlès, B., Gouriou, Y., and Chuchla, R.: On the circulation in the upper layer of the western equatorial Atlantic, Journal of Geophysical Research: Oceans, 104, 21 151–21 170, https://doi.org/10.1029/1999JC900058, 1999.

Bowden, K. F.: The dynamics of flow on a submarine ridge, Tellus, 12, 419–426, https://doi.org/10.3402/tellusa.v12i4.9415, 1960.

Brandt, P., Schott, F. A., Provost, C., Kartavtseff, A., Hormann, V., Bourlès, B., and Fischer, J.: Circulation in the central equatorial Atlantic: Mean and intraseasonal to seasonal variability, Geophysical Research Letters, 33, https://doi.org/10.1029/2005GL025498, 2006.

Brandt, P., Hormann, V., Körtzinger, A., Visbeck, M., Krahmann, G., Stramma, L., Lumpkin, R., and Schmid, C.: Changes in the ventilation of the oxygen minimum zone of the tropical North Atlantic, Journal of Physical Oceanography, 40, 1784–1801, https://doi.org/10.1175/2010JPO4301.1, 2010.

Bressac, M., Guieu, C., Doxaran, D., Bourrin, F., Desboeufs, K., Leblond, N., and Ridame, C.: Quantification of the lithogenic carbon pump following a simulated dust-deposition event in large mesocosms, Biogeosciences, 11, 1007–1020, https://doi.org/10.5194/bg-11-1007-2014.hal-00952676, 2014.

Brewer, P. G., Spencer, D. W., Biscaye, P. E., Hanley, A., Sachs, P. L., Smith, C. L., Kadar, S., and Fredericks, J.: The distribution of particulate matter in the Atlantic Ocean, Earth and Planetary Science Letters, 32, 393–402, https://doi.org/10.1016/0012-821X(76)90080-7, 1976.

Bruce, J., Kerling, J., and Beatty III, W.: On the North Brazilian eddy field, Progress in oceanography, 14, 57–63, https://doi.org/10.1016/0079-6611(85)90005-9, 1985.

Bubnova, E., Kapustina, M., Krechik, V., and Sivkov, V.: Suspended matter distribution in the surface layer of the East Equatorial Atlantic, Oceanology, 60, 228–235, https://doi.org/10.31857/S0030157420010049, 2020.

Burlakova, Z., Eremeeva, L., and Morozova, A.: Suspended matter in the estuaries of the Guinean shelf, Physical Oceanography, 8, 269–283, 1997.

Candela, J., Beardsley, R. C., and Limeburner, R.: Separation of tidal and subtidal currents in ship-mounted acoustic Doppler current profiler observations, Journal of Geophysical Research: Oceans, 97, 769–788, https://doi.org/10.1029/91JC02569, 1992.

Chester, R.: Particulate material in the oceans, in: Marine Geochemistry, pp. 321–345, Springer, https://doi.org/10.1007/978-94-010-9488-7{_10, 1990.

Craig, H. and Turekian, K.: The GEOSECS program: 1973–1976, Earth and Planetary Science Letters, 32, 217–219, https://doi.org/10.1016/0012-821X(76)90062-5, 1976.

Csanady, G.: "Pycnobathic" currents over the upper continental slope, Journal of physical oceanography, 15, 306–315, https://doi.org/10.1175/1520-0485(1985)015<0306:COTUCS>2.0.CO;2, 1985.

Didden, N. and Schott, F.: Eddies in the North Brazil Current retroflection region observed by Geosat altimetry, Journal of Geophysical Research: Oceans, 98, 20 121–20 131, https://doi.org/10.1029/93JC01184, 1993.

Doi, T., Tozuka, T., and Yamagata, T.: Interannual variability of the Guinea Dome and its possible link with the Atlantic Meridional Mode, Climate dynamics, 33, 985–998, https://doi.org/10.1007/s00382-009-0574-z, 2009.

Egloff, J.: Morphology of ocean basin seaward of northwest Africa: Canary Islands to Monrovia, Liberia, AAPG Bulletin, 56, 694–706, 1972.

Eittreim, S., Thorndike, E. M., and Sullivan, L.: Turbidity distribution in the Atlantic Ocean, Deep Sea Research and Oceanographic Abstracts, 23, 1115–1127, https://doi.org/10.1016/0011-7471(76)90888-3, 1976.

Eittreim, S. L. and Ewing, M.: Turbidity distribution in the deep waters of the western Atlantic trough, in: Suspended solids in water, pp. 213–225, Springer, 1974.

Emelyanov, E. M.: The barrier zones in the ocean, Springer Science & Business Media, 2005.

Emery, K. and Honjo, S.: Surface suspended matter off western Africa: relations of organic matter, skeletal debris and detrital minerals, Sedimentology, 26, 775–794, https://doi.org/10.1111/j.1365-3091.1979.tb00972.x, 1979.

Fratantoni, D. M., Johns, W. E., and Townsend, T. L.: Rings of the North Brazil Current: Their structure and behavior inferred from observations and a numerical simulation, Journal of Geophysical Research: Oceans, 100, 10 633–10 654, https://doi.org/10.1029/95JC00925, 1995.

Gardner, W. D., Biscaye, P. E., Zaneveld, J. R. V., and Richardson, M. J.: Calibration and comparison of the LDGO nephelometer and the OSU transmissometer on the Nova Scotian Rise, Marine Geology, 66, 323–344, https://doi.org/10.1016/0025-3227(85)90037-4, 1985a.

Gardner, W. D., Southard, J. B., and Hollister, C. D.: Sedimentation, resuspension and chemistry of particles in the northwest Atlantic, Marine Geology, 65, 199–242, https://doi.org/10.1016/0025-3227(85)90057-X, 1985b.

Gardner, W. D., Richardson, M. J., Mishonov, A. V., and Biscaye, P. E.: Global comparison of benthic nepheloid layers based on 52 years of nephelometer and transmissometer measurements, Progress in Oceanography, 168, 100–111, https://doi.org/10.1016/j.pocean.2018.09.008, 2018.

GEBCO Bathymetric Compilation Group, .: The GEBCO_2020 Grid–a continuous terrain model of the global oceans and land, https://doi.org/10.5285/a29c5465-b138-234d-e053-6c86abc040b9, 2020.

Gibbs, R. J.: The suspended material of the Amazon shelf and tropical Atlantic Ocean, in: Suspended solids in water, pp. 203–210, Springer, https://doi.org/10.1007/978-1-4684-8529-5{_1, 1974.

Herbland, A., Le Bouteiller, A., and Raimbault, P.: Size structure of phytoplankton biomass in the equatorial Atlantic Ocean, Deep Sea Research Part A. Oceanographic Research Papers, 32, 819–836, https://doi.org/10.1016/0198-0149(85)90118-9, 1985.

Iversen, M. H. and Ploug, H.: Ballast minerals and the sinking carbon flux in the ocean: carbon-specific respiration rates and sinking velocity of marine snow aggregates, Biogeosciences, 7, 2613–2624, https://doi.org/10.5194/bg-7-2613-2010, 2010.

Jeandel, C., van der Loeff, M. R., Lam, P. J., Roy-Barman, M., Sherrell, R. M., Kretschmer, S., German, C., and Dehairs, F.: What did we learn about ocean particle dynamics in the GEOSECS–JGOFS era?, Progress in Oceanography, 133, 6–16, https://doi.org/10.1016/j.pocean.2014.12.018, 2015.

Johns, W. E., Lee, T., Beardsley, R., Candela, J., Limeburner, R., and Castro, B.: Annual cycle and variability of the North Brazil Current, Journal of Physical Oceanography, 28, 103–128, https://doi.org/10.1175/1520-0485(1998)028<0103:ACAVOT>2.0.CO;2, 1998.

Karstensen, J., Stramma, L., and Visbeck, M.: Oxygen minimum zones in the eastern tropical Atlantic and Pacific oceans, Progress in Oceanography, 77, 331–350, https://doi.org/10.1016/j.pocean.2007.05.009, 2008.

Lal, D.: The oceanic microcosm of particles, Science, 198, 997–1009, https://doi.org/10.1126/science.198.4321.997, 1977.

Lavelle, J.: On the dynamics of current jets trapped to the flanks of mid-ocean ridges, Journal of Geophysical Research: Oceans, 117, 2012.

Lázaro, C., Fernandes, M. J., Santos, A. M. P., and Oliveira, P.: Seasonal and interannual variability of surface circulation in the Cape Verde region from 8 years of merged T/P and ERS-2 altimeter data, Remote sensing of environment, 98, 45–62, https://doi.org/10.1016/j.rse.2005.06.005, 2005.

Louis, J., Pedrotti, M. L., Gazeau, F., and Guieu, C.: Experimental evidence of formation of transparent exopolymer particles (TEP) and POC export provoked by dust addition under current and high p CO2 conditions, PloS one, 12, e0171 980, https://doi.org/10.1371/journal.pone.0171980, 2017.

Mayer, D. A. and Weisberg, R. H.: A description of COADS surface meteorological fields and the implied Sverdrup transports for the Atlantic Ocean from 30 S to 60 N, Journal of Physical Oceanography, 23, 2201–2221, https://doi.org/10.1175/1520-0485(1993)023<2201:ADOCSM>2.0.CO;2, 1993.

Mazarovich, A. and Sokolov, S. Y.: Hydrothermal fields in the Mid-Atlantic Ridge: Setting and prospects for further discoveries, Russian Journal of Earth Sciences, 4, 2002.

McCartney, M., Bennett, S., and Woodgate-Jones, M.: Eastward flow through the Mid-Atlantic Ridge at 11 N and its influence on the abyss of the eastern basin, Journal of Physical Oceanography, 21, 1089–1121, https://doi.org/10.1175/1520-0485(1991)021<1089:EFTTMA>2.0.CO;2, 1991.

McCartney, M. S.: Crossing of the equator by the deep western boundary current in the western Atlantic Ocean, Journal of physical oceanography, 23, 1953–1974, https://doi.org/10.1175/1520-0485(1993)023<1953:COTEBT>2.0.CO;2, 1993.

McCave, I.: Vertical flux of particles in the ocean, Deep Sea Research and Oceanographic Abstracts, 22, 491–502, https://doi.org/10.1016/0011-7471(75)90022-4, 1975.

McCave, I.: Particulate size spectra, behavior, and origin of nepheloid layers over the Nova Scotian continental rise, Journal of Geophysical Research: Oceans, 88, 7647–7666, https://doi.org/10.1029/JC088iC12p07647, 1983.

McCave, I.: Size spectra and aggregation of suspended particles in the deep ocean, Deep Sea Research Part A. Oceanographic Research Papers, 31, 329–352, https://doi.org/10.1016/0198-0149(84)90088-8, 1984.

McCave, I.: Properties of suspended sediment over the HEBBLE area on the Nova Scotian Rise, Marine Geology, 66, 169–188, https://doi.org/10.1016/0025-3227(85)90028-3, 1985.

McCave, I.: Local and global aspects of the bottom nepheloid layers in the world ocean, Netherlands Journal of Sea Research, 20, 167–181, https://doi.org/10.1016/0077-7579(86)90040-2, 1986.

McCave, I., Hall, I. R., Antia, A., Chou, L., Dehairs, F., Lampitt, R., Thomsen, L., Van Weering, T., and Wollast, R.: Distribution, composition and flux of particulate material over the European margin at 47–50 N, Deep Sea Research Part II: Topical Studies in Oceanography, 48, 3107–3139, https://doi.org/10.1016/S0967-0645(01)00034-0, 2001.

Mittelstaedt, E.: The ocean boundary along the northwest African coast: Circulation and oceanographic properties at the sea surface, Progress in Oceanography, 26, 307–355, https://doi.org/10.1016/0079-6611(91)90011-A, 1991.

Molinari, R. L., Fine, R. A., and Johns, E.: The deep western boundary current in the tropical North Atlantic Ocean, Deep Sea Research Part A. Oceanographic Research Papers, 39, 1967–1984, https://doi.org/10.1016/0198-0149(92)90008-H, 1992.

Morozov, E. G.: Oceanic Internal Tides: Observations, Analysis and Modeling, Cham: Springer International Publishing, https://doi.org/10.1007/978-3-319-73159-9, 2018.

Mullin, J. and Riley, J.: The colorimetric determination of silicate with special reference to sea and natural waters, Analytica chimica acta, 12, 162–176, 1955.

Nowell, A., McCave, I., and Hollister, C.: Contributions of HEBBLE to understanding marine sedimentation, Marine Geology, 66, 397–409, https://doi.org/10.1016/0025-3227(85)90041-6, 1985.

Oudot, C., Ternon, J.-F., Andrié, C., Braga, E. S., and Morin, P.: On the crossing of the equator by intermediate water masses in the western Atlantic Ocean: Identification and pathways of Antarctic Intermediate Water and Upper Circumpolar Water, Journal of Geophysical Research: Oceans, 104, 20 911–20 926, https://doi.org/10.1029/1999JC900123, 1999.

Passow, U.: Transparent exopolymer particles (TEP) in aquatic environments, Progress in oceanography, 55, 287–333, https://doi.org/10.1016/S0079-6611 (02)00138-6, 2002.

Passow, U. and Alldredge, A.: Distribution, size and bacterial colonization of transparent exopolymer particles (TEP) in the ocean, Marine Ecology Progress Series, pp. 185–198, 1994.

Passow, U., Shipe, R., Murray, A., Pak, D., Brzezinski, M., and Alldredge, A.: The origin of transparent exopolymer particles (TEP) and their role in the sedimentation of particulate matter, Continental Shelf Research, 21, 327–346, https://doi.org/10.1016/S0278-4343(00)00101-1, 2001.

Peterson, R. G. and Stramma, L.: Upper-level circulation in the South Atlantic Ocean, Progress in oceanography, 26, 1–73, https://doi.org/10.1016/0079-6611(91)90006-8, 1991.

Petschick, R., Kuhn, G., and Gingele, F.: Clay mineral distribution in surface sediments of the South Atlantic: sources, transport, and relation to oceanography, Marine Geology, 130, 203–229, https://doi.org/10.1016/0025-3227(95)00148-4, 1996.

Pradhan, Y., Lavender, S. J., Hardman-Mountford, N. J., and Aiken, J.: Seasonal and inter-annual variability of chlorophyll-a concentration in the Mauritanian upwelling: Observation of an anomalous event during 1998–1999, Deep Sea Research Part II: Topical Studies in Oceanography, 53, 1548–1559, https://doi.org/10.1016/j.dsr2.2006.05.016, 2006.

Reid, J. L.: On the total geostrophic circulation of the North Atlantic Ocean: Flow patterns, tracers, and transports, Progress in Oceanography, 33, 1–92, https://doi.org/10.1016/0079-6611(89)90001-3, 1994.

Reid, J. L.: On the total geostrophic circulation of the Pacific Ocean: Flow patterns, tracers, and transports, Progress in Oceanography, 39, 263–352, https://doi.org/10.1016/S0079-6611(97)00012-8, 1997.

Rhein, M., Stramma, L., and Krahmann, G.: The spreading of Antarctic bottom water in the tropical Atlantic, Deep Sea Research Part I: Oceanographic Research Papers, 45, 507–527, https://doi.org/10.1016/S0967-0637(97)00030-7, 1998.

Richardson, P., Hufford, G., Limeburner, R., and Brown, W.: North Brazil current retroflection eddies, Journal of Geophysical Research: Oceans, 99, 5081–5093, https://doi.org/10.1029/93JC03486, 1994.

Rossignol, M. and Meyrueis, A.: Campagnes oceanographiques du Gerad-Treca, Cent. Oceanogr. Dakar-Thiaroye, ORSTOM, Dakar, Senegal, 53, 1964.

Sarafanov, A., Sokov, A., and Demidov, A.: Water mass characteristics in the equatorial North Atlantic: A section nominally along 6.5 N, July 2000, Journal of Geophysical Research: Oceans, 112, https://doi.org/10.1029/2007JC004222, 2007.

Schlitzer, R.: Ocean Data View, https://odv.awi.de/, 2018.

Schott, F. A., Brandt, P., Hamann, M., Fischer, J., and Stramma, L.: On the boundary flow off Brazil at 5–10 S and its connection to the interior tropical Atlantic, Geophysical Research Letters, 29, 21–1, https://doi.org/10.1029/2002GL014786, 2002.

Sheldon, R., Prakash, A., and Sutcliffe Jr, W.: The size distribution of particles in the ocean 1, Limnology and oceanography, 17, 327–340, https://doi.org/10.4319/lo.1972.17.3.0327, 1972.

Siedler, G., Zangenberg, N., Onken, R., and Morlière, A.: Seasonal changes in the tropical Atlantic circulation: Observation and simulation of the Guinea Dome, Journal of Geophysical Research: Oceans, 97, 703–715, https://doi.org/10.1029/91JC02501, 1992.

Signorini, S., Murtugudde, R., McClain, C., Christian, J., Picaut, J., and Busalacchi, A.: Biological and physical signatures in the tropical and subtropical Atlantic, Journal of Geophysical Research: Oceans, 104, 18 367–18 382, https://doi.org/10.1029/1999JC900134, 1999.

Sivkov, V., Zhurov, Y., and Demidova, T.: A new data on the distribution of suspended matter in the North Atlantic, in: Proceedings of the XIV School of Marine geology, vol. 2, pp. 172–173, IO RAN, https://doi.org/In Russian, 2001.

Smith, K., Williams, P., and Druffel, E.: Upward fluxes of particulate organic matter in the deep North Pacific, Nature, 337, 724–726, https://doi.org/10.1038/337724a0, 1989.

Sokov, A., Morozov, E., Shapovalov, S., Borodkin, S., and Demidova, T.: Water structure in the equatorial Atlantic on the basis of the year 2000 transatlantic section, Oceanology, 42, 1–6, 2002.

Stramma, L. and Schott, F.: The mean flow field of the tropical Atlantic Ocean, Deep Sea Research Part II: Topical Studies in Oceanography, 46, 279–303, https://doi.org/10.1016/S0967-0645(98)00109-X, 1999.

Stramma, L., Rhein, M., Brandt, P., Dengler, M., Böning, C., and Walter, M.: Upper ocean circulation in the western tropical Atlantic in boreal fall 2000, Deep Sea Research Part I: Oceanographic Research Papers, 52, 221–240, https://doi.org/10.1016/j.dsr.2004.07.021, 2005.

Stramma, L., Brandt, P., Schafstall, J., Schott, F., Fischer, J., and Körtzinger, A.: Oxygen minimum zone in the North Atlantic south and east of the Cape Verde Islands, Journal of Geophysical Research: Oceans, 113, https://doi.org/10.1029/2007JC004369, 2008.

Thorpe, S. and White, M.: A deep intermediate nepheloid layer, Deep Sea Research Part A. Oceanographic Research Papers, 35, 1665–1671, https://doi.org/10.1016/0198-0149(88)90109-4, 1988.

Tucholke, B. E. and Eittreim, S.: The western boundary undercurrent as a turbidity maximum over the Puerto Rico Trench, Journal of Geophysical Research, 79, 4115–4118, 1974.

Turekian, K. K.: The fate of metals in the oceans, Geochimica et Cosmochimica Acta, 41, 1139–1144, https://doi.org/10.1016/0016-7037(77)90109-0, 1977.

Van der Jagt, H., Friese, C., Stuut, J.-B. W., Fischer, G., and Iversen, M. H.: The ballasting effect of Saharan dust deposition on aggregate dynamics and carbon export: Aggregation, settling, and scavenging potential of marine snow, Limnology and Oceanography, 63, 1386–1394, https://doi.org/10.1002/lno.10779, 2018.

Vladimirov, V., Bezborodov, A., Martynov, O., Ovsyanyi, E., and Diallo, B.: Relation between the depth of visibility of a white disk and the concentration of suspended matter in shelf waters off the Republic of Guinea, Soviet journal of physical oceanography, 1, 469–474, 1990.

Whitehead Jr, J. and Worthington, L.: The flux and mixing rates of Antarctic Bottom Water within the North Atlantic, Journal of Geophysical Research: Oceans, 87, 7903–7924, https://doi.org/10.1029/JC087iC10p07903, 1982.

Wilson, W. D., Johns, E., and Molinari, R.: Upper layer circulation in the western tropical North Atlantic Ocean during August 1989, Journal of Geophysical Research: Oceans, 99, 22 513–22 523, https://doi.org/10.1029/94JC02066, 1994.

Wüst, G.: Die Stratosphäre des Atlantischen Ozeans, Deutsche Atlantische Exped, Meteor 1925–1927, Wiss. Erg, 6, 288, 1935.